Peculiarities of gallium crystallization in confined geometry

© B.F. Borisov*, E.V. Charnaya*,**, A.V. Gartvik*, Cheng Tien**, Yu.A. Kumzerov***, V.K. Lavrentev****

* Institute of Physics, St. Petersburg State University,
198504 Petrodvorets, St. Petersburg, Russia
** Department of Physics, National Cheng Kung University,
70101 Tainan, Taiwan
*** A.F. Ioffe Physico-Technical Institute, Russian Academy of Sciences,
194021 St. Petersburg, Russia
**** Institute of High-Molecular Combinations,
199004 St. Petersburg, Russia

E-mail: charnaya@mail.ru

(Received 16 March 2004)

The freezing and melting phase transitions for gallium embedded into a porous glass with pore size of about 8 nm were studied using acoustic, NMR, and x-ray techniques. It was shown that the broadened solidification and melting transitions upon deep cooling until complete freezing at 165 K were due to formation of β-Ga within pores. The offset of confined β-Ga melting was lowered by about 21 K compared to the bulk β-Ga melting point. Both melting and freezing in pores were irreversible. The fulfillment of some special thermal conditions led to gallium crystallization into other modifications. The role of heterogeneous crystallization in freezing of confined gallium is discussed.

The present work was partially supported by the National Science Council of Taiwan under Grant 91-2112-M-006-017.

1. Introduction

Recently, a great deal of attention was focused on studies of surface and size effects induced by confined geometry. Properties of materials embedded into nanoporous matrices were shown to differ remarkably from those in bulk. In particular, metals confined within porous glasses and artificial opals manifest alterations in their superconducting behavior [1–3], atomic mobility in melted state [4], melting and freezing processes [5–9], electronic features [10] and in crystalline structure [11,12]. Studies of melting and freezing of metals in confined geometry revealed some common features such as noticeable reduction of the phase transition temperatures and rather reproducible thermal hysteresis upon cooling and warming. These changes in behavior of confined metals were similar to anomalies upon melting and freezing for simple and organic liquids within nanoporous matrices observed until now (see [13,14] and references therein). Some other properties were specific for melting and freezing in particular metals. For instance, acoustic and NMR measurements on mercury in porous glasses were treated within the model of liquid skin formed upon melting [7,8] similarly to melting of isolated metallic particles [15,16].

The melting and freezing processes of gallium in confined geometry were studied in [9,11,12] and in references therein. First NMR, acoustic, calorimetric and resistance measurements carried out for gallium embedded into artificial opals and porous glasses with 4 and 200 nm pore sizes revealed noticeable depression of the melting and freezing temperatures compared to the melting point of bulk α-gallium accompanied with pronounced hysteresis. The melting process was reported to be strongly broadened while freezing could be quite sharp. However, contrary to the case of confined mercury and other liquids, the hysteresis loops observed for gallium within most of porous matrices were complicated with two or more steps upon cooling and warming. Later x-ray studies showed that gallium in nanometer-size pores can crystallize into different modifications [11,12]. Note that bulk gallium also occurs in different crystalline phases [17,18]. Under ambient pressure, bulk liquid gallium crystallizes into α-Ga with the melting point of 303 K and the supercooled melt can freeze into β-Ga (the melting point 256.5 K). Other bulk crystalline modifications occur only under high pressure. Solid modifications of gallium submicrometric droplets coincide with the bulk ones [19]. According to [11,12,20] confined gallium modifications depended on pore size and geometry. They included the bulk α- and β-gallium as well as some modifications with symmetry different from known bulk gallium structures. In particular, a tetragonal modification [11] was observed in artificial opals and in porous glasses with pore size of 4 nm. Polymorphism of confined gallium explained the complex character of its freezing and melting transitions. However, the processes of simultaneous or consecutive crystallization into various modifications and their interrelation with pore geometry and thermal history are not clear until now. The reduction of the gallium phase transition temperatures and irreversible melting agreed according to [9,11] with predictions of the Gibbs–Thompson equation developed for isolated small spherical particles. Nevertheless, the coexistence within pores of various crystalline species along with their structure disordering and some other experimental facts discussed in [11,12] prevented the quantitative treatment. Another aspect of gallium solidification

which was discussed in [9,11,12] concerned the nature of nucleation (homogeneous or heterogeneous) in confined geometry and reasons for thermal hysteresis upon cooling and warming. While experimental results obtained in [9] allowed suggesting the significant role of hetergeneous crystallization within pores, the matter remained unclear until now.

The aim of the present paper is to study using acoustic, NMR, and x-ray methods the melting and freezing processes for gallium in a porous glass with about 8 nm pores in connection with the problems stated above.

2. Experimental

Samples of porous glass used in the present work were prepared of phase-separated soda borosilicate glass with pore structure produced by acid leaching. The pore size found to be equal to 8.4 nm by mercury intrusion porosimetry and small angle x-ray scattering. The pore volume distribution versus pore diameter according to mercury porosimetry is shown in Fig. 1. The liquid gallium was introduced into pores under high pressure up to 10 kbar. The filling factor of the pore volume was near 85%.

Numerous acoustic investigations of porous matrices filled with liquids showed that the velocity of longitudinal as well as transverse ultrasonic waves changes noticeably upon melting or greezing of embedded materials following changes in effective elastic moduli of the samples [7–9,21,22]. This allows the use of acoustic methods for detailed studies of the melting and freezing processes in confined geometry. We employed the conventional pulse ultrasound technique [23] at the frequency of 7 MHz, which gave the relative longitudinal sound velocity value

$$\Delta v/v = \big[v(T) - v(T = 295\,\mathrm{K})\big]/v(T = 295\,\mathrm{K})$$

with an accuracy better than 10^{-5}. All measurements were made during continuous slow cooling or warming the sample within a range 295 to 160 K with various rates of changing temperature. The temperature gradient in the sample did not exceed 0.05 K/cm.

NMR measurements were carried out using a pulse Bruker Avance 400 NMR spectrometer. The ^{71}Ga NMR signal corresponding to liquid gallium was observed at various stabilized temperatures in the range 295 to 160 K. Since the integral intensity of the signal is proportional to the total amount of melted gallium, NMR provides direct information on the fraction of liquid and solid gallium phases within pores. The operating frequency was 122 HMz. The temperature was controlled within 0.5 K. Prior to each measurement, the sample was kept at a fixed temperature for about 5 minutes. To detect NMR line, a single pulse sequence with phase cycling was applied with pulse duration of 2.5 μs. The repetition time was 0.1 s.

The x-ray diffraction measurements were performed using a commercial powder diffractometer DRON-2.0 with Cu$K\alpha$ radiation at several temperatures between 180 and 295 K. During measurements the temperature was stable within 2 K. The x-ray patterns were recorded within an angle range 20 to 80 degrees with the scan speed of 0.5 deg/min.

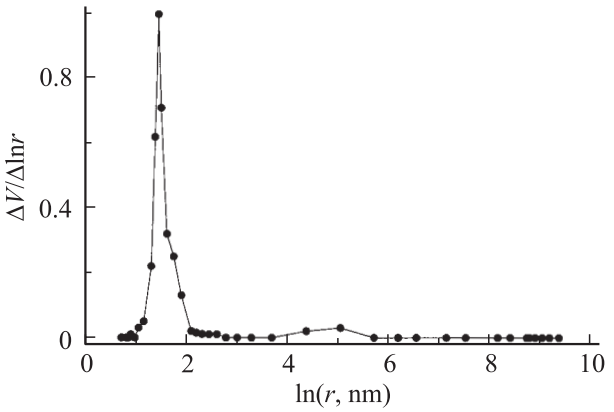

Figure 1. Pore zise distribution in the porous glass under study according to mercury intrusion porosimetry.

3. Results and discussion

Temperature dependence of intensity of ^{71}Ga NMR line corresponding to liquid gallium upon cooling from room temperature down to 160 K and consecutive warming for the rate of changing temperature between measurements of about 50 K/h is presented in Fig. 2. It shows that confined gallium starts freezing at about 215 K and the solidification process ends at about 165 K. Upon warming, the melting process becomes noticeable only above 195 K and the total amount of gallium melts near 235 K. Note that smooth alterations in the NMR signal intensity outside

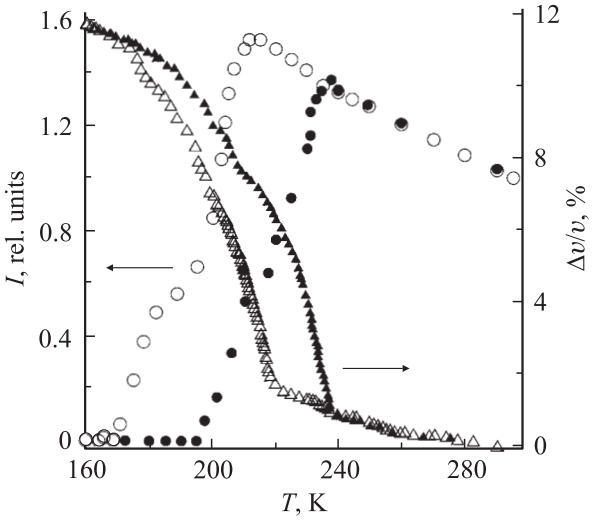

Figure 2. Temperature dependences of the NMR signal intensity I (circles) and relative ultrasound velocity $\Delta v/v$ (triangles) for the full freezing-melting thermocycle upon cooling (open symbols) and warming (closed symbols).

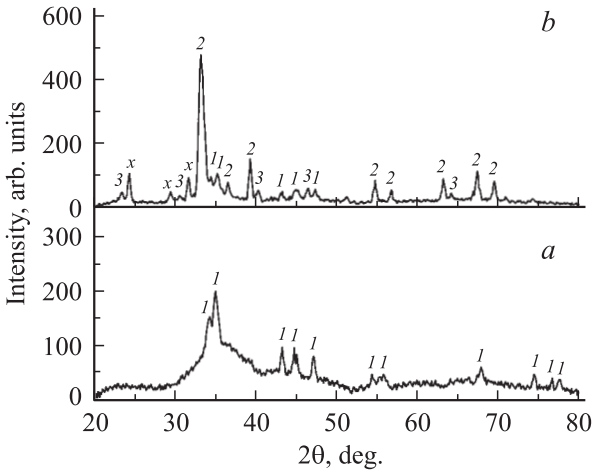

Figure 3. *X*-ray powder diffraction patterns obtained at 211 K (*a*) upon cooling from room temperature and at 220 K (*b*) after consecutive cooling down from room temperature to 205 K, warming up to 240 K, cooling down to 190 K, and warming up to 220 K. Peaks corresponding to β-Ga, the tetragonal modification, α-Ga and to a unidentified structure are marked with *1*, *2*, *3* and *x*, respectively.

of the gallium phase transitions obviously rise due to the Curie law for nuclear susceptibility. The full hysteresis loops upon cooling and warming with similar rate of changing temperature were quite reproducible, the temperatures of the onset and offset of the phase transformations shifted for no more than several degrees. Measurements of temperature dependences of ultrasound velocity for similar thermocycles also showed hysteresis loops associated with the melting and freezing processes (Fig. 2) which agreed well with the NMR data.

As can be seen in Fig. 2, both the melting and freezing processes are noticeably lowered compared to those for bulk α-Ga and smeared over large temperature ranges. *X*-ray measurements showed that the freezing observed is related with formation within pores of a single crystalline modification coincided with β-Ga. The *x*-ray pattern obtained at 211 K after cooling from room temperature is shown in Fig. 3, *a*.

The width of peaks in Fig. 3, *a* was greater than the instrumental broadening (0.3°). Hence, following [11,12] one can evaluate the average size of confined metallic crystallites from the peak broadening using the Scherrer equation [24]. The obtained size of about 25 nm is noticeably larger than the pore diameter. This means that the crystallization front passes through gallium within several neighbor pores. Similar difference in pore diameters and crystallite sizes was also found for gallium in other nanoporous matrices [11,12], for indium in Vycor glass [5] and for some wetting liquids such as O_2, D_2 and CO_2 (see [25] and references therein) in contrast to confined mercury [6].

Using acoustic methods we then performed detailed studies of influence of the rate of changing temperature and of thermal history on the melting and freezing processes for confined gallium. The measurements disclosed that, when thermocycles started at room temperature and cooling continued down to below 204 K, the main hysteretic behavior was reproducible independently of the cooling or warming rate. Namely, freezing started near 215 K and the offset of melting was seen near 235 K. It was also obtained that both melting and freezing were completely irreversible, that is when crystallization was interrupted at some intermediate temperature and the sample under study was warmed up, the velocity curve upon warming did not coincide with that upon cooling but merged with the warming branch of the full hysteresis loop at higher temperatures. An example is shown in Fig. 4, *a*. Similarly, when the sample was cooled down after incomplete melting, the velocity curve tended to merge with the cooling branch of the full hysteresis loop. Note, that the irreversible freezing in confined geometry was also seen in other liquids [7,13,22] and can be explained by hysteresis between freezing and melting. However, a temperature range of reversible melting was found upon warming for some liquids in porous matrices including mercury [7,8,13] contrary to the results obtained for gallium in the present and previous studies.

Normally the treatment of the melting and freezing phase transitions for confined liquids is based on models developed for isolated spherical or cylindrical particles [8,13,21,22]. Simple theories predict reduction of the melting or freezing points for small paticles because of a large surface to volume ratio. For spherical paticles the melting temperature depression ΔT_m is given by the Gibbs–Thompson equation [26]

$$\Delta T_m = 2\gamma v_0 T_b / Lr, \qquad (1)$$

where r is the particle radius, γ is the surface tension of the solid, L — is the latent heat of fusion, T_b is the bulk melting temperature, and v_0 is the molar volume of the solid. Freezing is mostly treated as a result of supercooling. This explains the hysteresis between solidification and melting and therefore, the irreversible behavior upon freezing. However the geometric-freezing model was also discussed for porous media [22,27]. According to this model, crystallization in confined particles is considered similarly to structural phase transformations in solids. Then it is controlled by pore geometry and the depression of the freezing temperature ΔT_f for spherical particles is given by

$$\Delta T_f = 3\alpha v_0 T_b / Lr, \qquad (2)$$

where α is the surface energy. However, the geometric-freezing model can not provide an appropriate explanation for the hysteresis. A more complicated analysis implies the formation of a liquid layer (liquid skin) surrounding the solid core of a small particle (see [16,28] and references therein).

The relationships (1) and (2) predict that the phase transitions occur at a temperature determined by the particle radius. Thus the total processes in confined geometry should

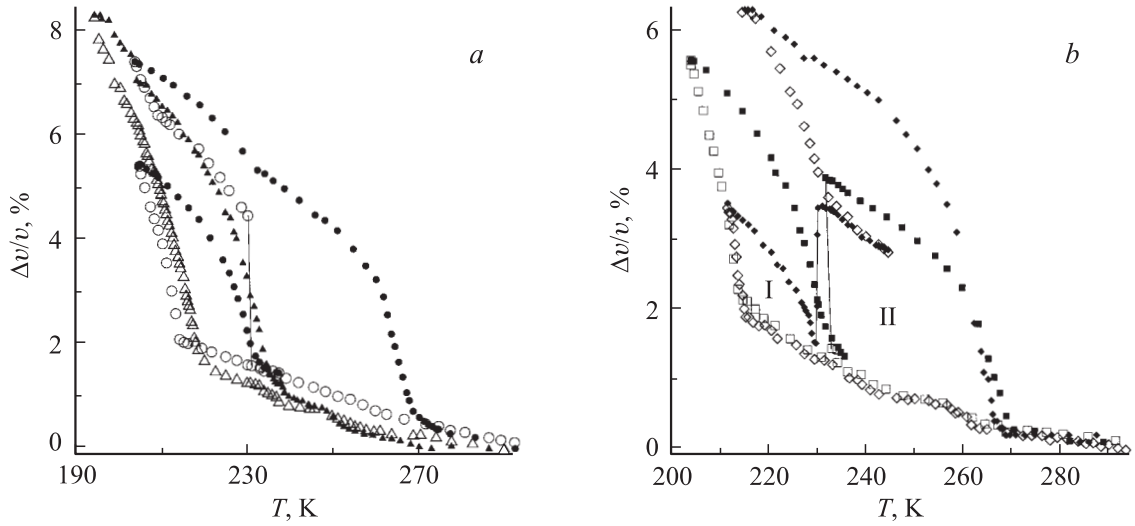

Figure 4. Temperature dependences of the relative ultrasound velocity $\Delta v/v$ upon cooling (open symbols) and warming (closed symbols) for thermocycles started at room temperature. The straight lines are guides for the eye. *a*) Triangles: cooling down to 194.4 K, warming up to room temperature. Circles: cooling down to 204.7 K, warming up to 237.2 K, cooling down to 203.7 K, and warming up to room temperature. *b*) Diamonds: cooling down to 204.4 K, warming up to 235.5, cooling down to 232 K, and warming up to room temperature. Squares: cooling down to 211.8 K, warming up to 245 K, cooling down to 215 K, and warming up to room temperature.

be irreversible and distribution of particle sizes should result in the phase transition broadening. Such an idea was used in some studies to find pore size distribution from melting processes of cyclohexane [14]. On the other hand, the liquid skin model predicts that the melting process of a particular particle occurs within a temperature range where the liquid layer becomes thicker [28]. Within this range, melting should be reversible until the offset point when the solid core melts. Therefore, the absence of the reversible melting range upon warming for gallium allows us to suggest that the liquid skin model is not applicable to confined gallium contrary to confined mercury and isolated metallic particles [7,15,16] or the melting broadening due to pore size distribution is much more essential then the smearing due to liquid layer formation.

According to Fig. 1 both the onset of freezing and the offset of melting for confined β-gallium are shifted to low temperatures compared to the melting point of bulk β-Ga. The lowering of the offset of melting is about 21 K while for β-Ga within pores in the opal [11] it was near 10 K. Since the pore sizes for the opal can be estimated as 50 and 100 nm [11], this result qualitatively agrees with predictions of the Gibbs–Thompson equation. Taking into account the irregular shape of confined particles, affected by pore geometry, and particle interconnection, one can hardly expect the precise accordance. Note, also, that the temperatures of the onset of freezing are almost the same in the porous glass under study and in the opal (about 215 K).

Acoustic studies also showed that the fulfillment of special conditions of thermocycling could change drastically the total process of gallium crystallization. For instance, when the sample was cooled down to a temperature lying below the onset of freezing, then consecutively warmed up to 237.2 K and again cooled down, the velocity manifested a jump just below the offset of melting in full thermocycles (Fig. 4). After the jump, the velocity branches corresponding to cooling and warming merged together only near 270 K (Fig. 4). The effect was quite reproducible. As it has been found in previous acoustic studies of melting and freezing in confined liquids, including confined metallic melts, the increase in ultrasound velocity reveals the process of crystallization within pores [7–9,21,22]. Thus, the abrupt increase in ultrasound velocity observed near 230 K can be treated as crystallization into another gallium modification (or several modifications) with the offset of melting at about 270 K. It should be noted that gallium crystallizes near 230 K only partially. The rest part of gallium remains liquid and freezes at lower temperatures as can be seen in Fig. 4.

To confirm the suggestion about gallium crystallization into modifications different from β-Ga we carried out additional x-ray studies. The x-ray pattern obtained at 220 K after a thermocycle corresponding to the conditions described above revealed additional peaks (Fig. 3, *b*). Most intense peaks (marked with *2*) coincided with those belonged to a tetragonal modification found recently in porous glass with pores of 4 nm and in artificial opals [11,12]. According to [29] it has the lattice parameters $a = 3.25$ Å, $c = 4.95$ Å and differs from known bulk gallium structures [18]. Using the lattice parameters a and c we can estimate the crystal density ρ assuming that the unit cell contains 3 atoms: $\rho = 6.65\,\mathrm{g/cm^3}$. The value obtained is larger than the density of liquid gallium ($\rho = 6.095\,\mathrm{g/cm^3}$) similarly to other known gallium modifications except the solid α-phase ($\rho = 5.91\,\mathrm{g/cm^3}$) [17,18]. Weaker peaks (marked with *3* in Fig. 3, *b*) can be attributed to the disordered α-phase

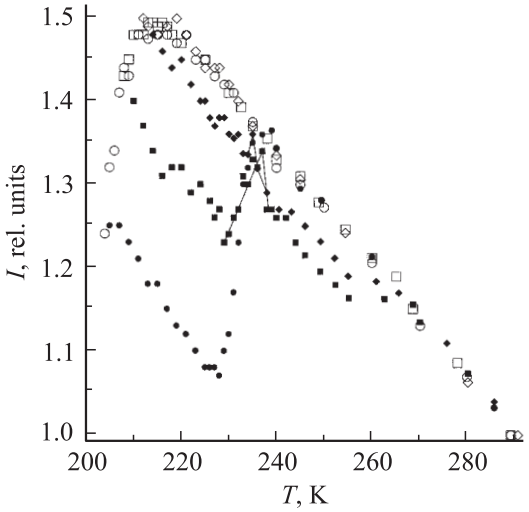

Figure 5. Temperature dependences of the NMR signal intensity I for three thermocycles started at room temperature. Circles — cooling down to 204 K, squares — to 208 K, diamonds — to 212 K. Open and closed symbols correspond to cooling and warming, respectively. The straight lines are guides for the eye.

following x-ray data published in [11] for gallium embedded into artificial opals. Three other peaks (marked with x) were not identified. Thus, according to the x-ray data obtained, the hysteresis loop I in Fig. 4, b arises due to formation of β-Ga while the hysteresis loop II is related chiefly with crystallization into the tetragonal modification and to a lesser extent into α-Ga and into a unidentified phase.

According to acoustic studies, freezing at about 230 K into the tetragonal and α modifications could also occur when the sample was cooled down to a temperature lying below the onset of freezing and 204 K (with the rate less than 15 K/h below about 235 K and less than 40 K/h at other temperatures) and consecutively warmed (Fig. 4, b). It should be expected that the decrease in the total amount of liquid gallium caused by partial crystallization at about 230 K can be detected by NMR. While precise enough NMR measurements need a long time due to large number of acquisitions and it is not easy to fulfill the necessary conditions, we obtained results, which agreed with the results of acoustic studies (Fig. 5). The crystallization was seen via the decrease in the total amount of liquid gallium near 235–238 K in contrast to the results observed after deeper cooling. Note that according to Fig. 5, the amount of additional gallium modification is rather small compared to alterations in ultrasound velocity. This difference could arise due to some variations in thermal conditions during NMR and acoustic measurements. It is also neccessary to take into account that relative sensitivity of velocity to gallium freezing within pores depends on elastic properties of particular crystalline modifications.

The results obtained showed that while gallium confined within the porous glass under study normally starts freezing near 215 K, liquid gallium in pores is in a metastable state at higher temperatures and can crystallize under some conditions. Such peculiar features of confined gallium are related to its ability to occur in several different crystalline modifications, which melt at particular temperatures, and with its tendency to supercooling. Rather similar behavior could be seen in bulk gallium. When gallium is supercooled at ambient pressure well below the α-Ga melting point, it can crystallize into β-Ga [17]. It is also known that supercooled bulk gallium crystallizes below 303 K into the α modification upon cooling as well as upon warming if heterogeneous nucleation was initiated. The fact that the process of additional crystallization in confined gallium at about 230 K was observed only after preparatory cooling below the onset of ordinal freezing near 215 K (Fig. 4) shows the importance of the presence in pores of a small amount of frozen gallium. One can suggest that such crystallites serve as nucleation centers, which provoke heterogeneous crystallization. One can also suggest that thermal conditions used in the present studies influence the geometry and number of crystallites to make possible the crystallization near 230 K.

In conclusion, studies of freezing and melting for gallium confined within a porous glass with 8 nm pore size showed that the solidification and melting transitions upon deeper cooling until complete freezing started at about 215 K are due to formation of β-Ga within pores. The melting and freezing temperature ranges were noticeably down shifted compared to the bulk β-Ga melting point. Both melting and freezing were irreversible. The irreversibility of melting contradicts the liquid skin model and allows suggesting that the melting process broadening arises mainly due to pore size distribution, contrary to the case of confined mercury. The results obtained also revealed that fulfilling some special thermal conditions leads to gallium crystallization at about 230 K into the tetragonal gallium modification which was found intil now only in confined geometry and into the disordered α phase. The fact that the crystallization needs in some amount of crystallites of another confined gallium modification to start, evidences an important role of heterogeneous nucleation in freezing within pores.

References

[1] M.J. Graf, T.E. Huber, C.A. Huber. Phys. Rev. B **45**, 3133 (1992).
[2] E.V. Charnaya, C. Tien, K.J. Lin, Yu.A. Kumzerov, C.-S. Wur. Phys. Rev. B **58**, 467 (1998).
[3] C. Tien, C.-S. Wur, K.J. Lin, E.V. Charnaya, Yu.A. Kumzerov. Phys. Rev. B **61**, 14 833 (2000).
[4] E.V. Charnaya, T. Loeser, D. Michel, C. Tien, D. Yaskov, Yu.A. Kumzerov. Phys. Rev. Lett. **88**, 097 602 (2002).
[5] K.M. Unruh, T.E. Huber, C.A. Huber. Phys. Rev. B **48**, 9021 (1993).
[6] Yu.A. Kumzerov, A.A. Nabereznov, S.B. Vakhrushev, B.N. Savenko. Phys. Rev. B **52**, 4772 (1995).
[7] B.F. Borisov, E.V. Charnaya, P.G. Plotnikov, W.-D. Hoffmann, D. Michel, Yu.A. Kumzerov, C. Tien, C.S. Wur. Phys. Rev. B **58**, 5329 (1998).

[8] E.V. Charnaya, P.G. Plotnikov, D. Michel, C. Tien, B.F. Borisov, I.G. Sorina, E.I. Martynova. Phys. B **299**, 56 (2001).
[9] B.F. Borisov, E.V. Charnaya, T. Loeser, D. Michel, C. Tien, C.S. Wur, Yu.A. Kumzerov. J. Phys.: Condens. Matter **11**, 10 259 (1999).
[10] E.V. Charnaya, D. Michel, C. Tien, Yu.A. Kumzerov, D. Yaskov. J. Phys.: Condens. Matter **15**, 5469 (2003).
[11] E.V. Charnaya, C. Tien, K.J. Lin, Yu.A. Kumzerov. J. Phys.: Condens. Matter **10**, 7273 (1998).
[12] E.V. Charnaya, C. Tien, K.J. Lin, Yu.A. Kumzerov. Phys. Rev. B **58**, 11 089 (1998).
[13] H.K. Christenson. J. Phys.: Condens. Matter **13**, R95 (2001).
[14] J.H. Strange, M. Rahan, E.G. Smith. Phys. Rev. Lett. **71**, 3589 (1993).
[15] L. Gråbek, J. Bohr, H.H. Andersen, A. Johansen, E. Johnson, L. Sarholt-Kristensen, I.K. Robinson. Phys. Rev. B **45**, 2628 (1992).
[16] T. Ben David, Y. Lereah, G. Deutsher, R. Kofman, P. Cheyssac. Phil. Mag. A **71**, 1135 (1995).
[17] Chemistry of aluminum, gallium, indium and thallium / Ed. by A.J. Downs. Blackie Academic and Profeccional, London (1993).
[18] Powder Diffraction File, Inorganic Phases. International Centre for Diffraction Data, Newtown Square, PA (1992).
[19] A. Di. Cicco. Phys. Rev. Lett. **81**, 2942 (1998).
[20] C. Tien, C.S. Wur, K.J. Lin, J.S. Hwang, E.V. Charnaya, Yu.A. Kumzerov. Phys. Rev. B **54**, 11 880 (1996).
[21] C.L. Jackson, G.B. McKenna. J. Chem. Phys. **93**, 9002 (1990).
[22] E. Molz, A.P.Y. Wong, M.H.W. Chan, J.R. Beamish. Phys. Rev. B **48**, 5741 (1993).
[23] J. Williams, J. Lamb. J. Acoust. Soc. Am. **30**, 308 (1958).
[24] B.E. Warren. *X*-ray diffraction. Addison–Wesley, Reading, MA (1989).
[25] D.W. Brown, P.E. Sokol, A.P. Clarke, M.A. Alam, W.J. Nuttall. J. Phys.: Condens. Matter **9**, 7317 (1997).
[26] Ph. Buffat, J.-P. Borrel. Phys. Rev. A **13**, 2287 (1976).
[27] J. Warnock, D.D. Awschalom, M.W. Shafer. Phys. Rev. Lett. **57**, 1753 (1986).
[28] R.R. Vanfleet, J.M. Mochel. Surf. Sci. **341**, 40 (1995).
[29] I.G. Sorina, E.V. Charnaya, L.A. Smirnov, Yu.A. Kumzerov, C. Tien. Phys. Solid State **40**, 1407 (1998).